Blind separation of multichannel electrogastrograms using independent component analysis based on a neural network

Z. S. Wang[1] J. Y. Cheung[2] J. D. Z. Chen[1]

[1] Lynn Institute for Healthcare Research, 5300 N. Independence Ave., Suite 130, Oklahoma City, OK 73112, USA

[2] Department of Electrical & Computer Engineering, University of Oklahoma, OK, USA

Abstract—*The electrogastrogram (EGG) is an abdominal surface measurement of gastric myo-electrical activity which regulates gastric contractions. It is of great clinical importance to record and analyse multichannel EGGs, which provide more information on the propagation and co-ordination of gastric contractions. EGGs are, however, contaminated by myo-electric interference from other organs and artefacts such as motion and respiration. The aim of the study is to separate the gastric signal from noisy multichannel EGGs without any information on the interference, using independent component analysis. A neural-network model is proposed, and corresponding unsupervised learning algorithms are developed to achieve the separation. The performance of the proposed method is investigated using artificial data simulating real EGG signals. Experimental EGG data are obtained from humans and dogs. The processed results of both simulated and real EGG data show the following: first, the proposed method is able to separate normal gastric slow waves from respiratory artefacts and random noises. It is also able to extract gastric slow waves, even when the EGG is contaminated by severe respiratory and ECG artefacts. Secondly, when the stomach contains various gastric electric signals with different frequencies, the proposed method is able to separate these different signals, as illustrated by simulations. These data suggest that the proposed method can be used to separate gastric slow waves, respiratory and motion artefacts, and intestinal myo-electric interference that are mixed in the EGG. It can also be used to detect gastric slow-wave uncoupling, during which the stomach has multiple gastric signals with different frequencies. It is believed that the proposed method may also be applicable to other biomedical signals.*

Keywords—*Electrogastrogram, Blind source separation, Independent component analysis, Neural network*

Med. Biol. Eng. Comput., 1999, **37**, 80–86

1 Introduction

SINCE ALVAREZ'S creative work (1922), it has been extensively reported that, just as in the heart, there exists an electrophysiological process in the smooth muscle of the stomach, which is known as gastric myo-electric activity (GMA) and can be recorded *in vivo* with electrodes implanted in the serosa of the stomach. It is known that the function of GMA is to modulate the motility of the stomach (SARNA, 1975; CHEN and MCCALLUM, 1994).

GMA consists mainly of two components. One is electrical control activity (ECA), or basic electrical rhythm (BER), which is an omnipresent slow wave with a frequency of 3 cycles $\min^{-1}$ in healthy humans. The other is electrical response activity (ERA), which is the spike cluster or fast wave superimposed on the ECA (SARNA, 1975). The former reflects the maximum frequency of the contractions of the stomach, and the latter is associated with the appearance of contractions (SARNA, 1975; FAMILONI *et al.*, 1987; KOCH *et al.*, 1987; CHEN and MCCALLUM, 1993).

GMA can be cutaneously measured by placing surface electrodes on the abdomen over the stomach; this method is termed electrogastrography, and the surface signal obtained is called an electrogastrogram (EGG) (ALVAREZ, 1922; SMOUT *et al.*, 1980; FAMILONI *et al.*, 1987; KOCH *et al.*, 1987; ABEL and MALAGELADA, 1988; CHEN and MCCALLUM, 1993; 1994; MINTCHEV *et al.*, 1993). Owing to its non-invasive nature and capacity to reflect the major features of internal GMA, electrogastrography has become an attractive tool for physiological and pathophysiological studies of the stomach (SMOUT *et al.*, 1980; FAMILONI *et al.*, 1987; KOCH *et al.*, 1987; CHEN and MCCALLUM, 1993; 1994). The clinical significance of the EGG has been validated. For instance, it has been reported that

Correspondence should be addressed to Dr J. D. Z. Chen; email: jchen1@ecn.ou.edu

First received 9 March 1998 and in final form 13 July 1998

the EGG has a close relationship with gastric motor disorders and gastro-intestinal symptoms, such as nausea, vomiting and gastroparesis resulting from delayed gastric emptying (FAMILONI *et al.*, 1987; CHEN and MCCALLUM, 1993; 1994; CHEN *et al.*, 1996).

EGG is now on the verge of becoming a new clinical tool in gastro-enterology, but is not yet in extensive clinical use, unlike electrocardiograms (ECGs) (SMOUT *et al.*, 1980; CHEN and MCCALLUM, 1993; 1994; MINTCHEV *et al.*, 1993). One of the problems is that the EGG is weak in energy, very low frequency, sometimes of poor quality and vulnerable to various kinds of artefact, such as respiration and motion, especially compared with other electrophysiological signals, such as ECGs and EMGs (MINTCHEV *et al.*, 1993; LIANG *et al.*, 1997). Thus, a way to obtain higher-quality EGG data is an objective sought by researchers in the methodology field related to electrogastrography.

Instruments for measuring the EGG are equipped with lowpass filters to eliminate various kinds of interference from the measurement environment. However, the frequencies of some types of interference, such as motion artefacts and other noise, often overlap with that of the EGG, and thus lowpass filtering is not sufficient to eliminate all artefacts or random noise. Another possible way to improve EGG quality is the use of adaptive noise cancellation (ANC) technology, based on adaptive signal processing theory (VAN DER SCHEE *et al.*, 1981; CHEN *et al.*, 1989), by which noise is removed from the EGG through a subtraction and optimisation process. However, ANC requires a reference signal that is the comprehensive signal of the various artefacts to be removed. Obviously, it is difficult and sometimes unrealistic to obtain such a reference signal in practical applications, because artefacts are variable, and their distribution natures are unknown. Recently, a novel method to detect motion artefacts in the EGG was reported (LIANG *et al.*, 1997), using feature analysis and neural networks to detect and eliminate the motion artefacts. In this method, however, the contaminated signal segment is also deleted, together with the identified motion artefacts.

A new method for the measurement of multichannel EGG data using an electrode array was recently developed (ZHOU *et al.*, 1997). Obviously, such measurement has excellent potential for improving the quality of the EGG, and such multichannel data can provide us with more information on the internal GMA than the single-channel EGG. Owing to the mixing effects resulting from the transferring media and various kinds of artefact, however, these multichannel recordings are statistically correlated with one another. The question is how effectively to extract valuable information from such multichannel EGG or, at least, how to make best use of these multichannel recordings to extract or separate out cleaner signals that reflect the internal GMA more accurately.

The aim of this paper is to answer these questions. First of all, we will make clear the problem we are facing. As no one has a good way to obtain clean or 'original' GMA data from the abdominal surface, such an hypothesis is tenable, i.e. practical multichannel EGG signals are some kinds of mixture resulting from the true transferred GMA components and various kinds of noise or artefacts. However, there are questions as to what the 'true' components are and whether we can make it clear how they are mixed. The answer is probably 'no'. That is, the extraction of valuable or 'true' information from cutaneously recorded multichannel EGGs is a blind problem. Fortunately, a novel signal processing technology, blind signal processing, and especially blind source separation (BSS), has recently been developed (JUTTERN and HERAULT, 1991; SOROUCHYARI, 1991; BUREL, 1992; COMON, 1994; HYVARINEN, 1996), its application to biomedical signal analysis has been reported (MAKEIG and BELL, 1997), and it can be used to solve our problem.

In this paper, a blind separation method for multichannel EGGs using neural network-based independent component analysis (ICA) is presented. ICA is an effective technology for BSS, by which both first-order and second-order correlations among given multichannel signals can be removed and, when the source signals are statistically independent, they can be recovered from their linearly mixed versions. We proposed a neural network and a corresponding unsupervised learning algorithm for the implementation of the ICA. The experimental results showed that using this technology, the cleaner components can be separated from the multichannel EGG data contaminated by measurement artefacts, such as respiratory, motion and ECG, without any prior information on such contamination. The method can also be applied to other biomedical signals, such as ECG, EEG and EMG.

2 Methods

2.1 *Problem formulations*

ICA is a recently developed technology that expresses a set of random variables as linear combinations of statistically independent component variables (JUTTERN and HERAULT, 1991; SOROUCHYARI, 1991; BUREL, 1992; COMON, 1994; HYVARINEN, 1996). The promising applications of ICA are in blind source separation, feature extraction and blind deconvolution and so on. In the framework of ICA introduced by COMON (1994), we observe m signals $v_1(t), v_2(t), \ldots, v_m(t)$; for example, we measure m EGG signals using m channels, and these m signals are linear combinations of n unknown (blind) components $s_1(t), s_2(t), \ldots, s_n(t)$, which are assumed mutually statistically independent, i.e. their joint probability distribution function can be decomposed as

$$p(s) = \prod_{i=1}^{n} p_i(s_i) \tag{1}$$

where $p_i(s_i)$ is the probability density function (PDF) of the ith source signal, for example, one true EGG component and n-1 interference components. Such a linear relationship can be compactly represented as

$$v(t) = \sum_{i}^{n} \boldsymbol{a}_i s_i(t) = \boldsymbol{A}s(t) \tag{2}$$

where $v(t) = (v_1(t), v_2(t), \ldots, v_m(t))^T$ is the observation vector; $\boldsymbol{s}(t) = (s_1(t), s_2(t), \ldots, s_n(t))^T$ is the source vector; and A is an unknown (blind) $m \times n$ non-singular matrix not depending on time t, called the mixing matrix. The basic problem of ICA is to estimate the true source $s(t)$ from the mixed observation vector $\boldsymbol{v}(t)$, or, say, to estimate the inverse of the mixing matrix A. If we obtain a good estimator $\tilde{A}$ of A^{-1} only based on the observation vector $v(t)$, the source signals can be recovered by

$$\hat{s}(t) = \tilde{A}v(t)$$

2.2 *Data pre-processing and whitening*

Now that A and $s(t)$ are blind, we need to do some preliminary work on the only data $v(t)$, so that the blind separation task becomes easier. The preliminary work usually includes removing mean and whitening. The data whitening can be implemented by linearly transforming $v(t)$ into $\boldsymbol{x}(t)$, i.e.

$$\boldsymbol{x}(t) = \boldsymbol{U}v(t) \tag{3}$$

such that the correlation matrix of $x(t)$ becomes unit matrix $E\{x(t)x(t)^T\} = I$ ($E\{\cdot\}$ denotes the mathematics expectation of a random variable), which can be accomplished by classical principal component analysis (PCA). After whitening, we obtain

$$x(t) = Bs(t) \tag{4}$$

where $B = UA$ is an orthogonal matrix, because $E\{x(t)x(t)^T\} = BE\{s(t)s(t)^T\}B^T = BB^T = I$, where $E\{s(t)s(t)^T\} = I$, as we have assumed that $s(t)$ is statistically independent and has a zero mean. Now we have reduced the problem of finding an arbitrary matrix A to a simpler problem of finding an orthogonal matrix B. Once B is found, $s(t)$ can be computed by

$$s(t) = B^T x(t) = B^T Uv(t) \tag{5}$$

Eq. (5) is the key to solving the BSS problem, in which only the vector $v(t)$ is known and denotes measured multichannel signals, for example, multichannel EGG recordings. In the following, we will describe how to find the whitening matrix U (Section 2.3) and the orthogonal matrix B (Section 2.4), so that the unknown source signal vector $s(t)$ can be recovered from $v(t)$.

2.3 *Simple neural learning algorithm for PCA*

The PCA whitening $n \times m$ matrix U in Eqn. 5 is obtained using the following simple neural learning algorithm:

$$U_{k+1} = U_k - \mu_k[v(t)v(t)^T - I]U_k \tag{6}$$

where k denotes the learning time, and μ_k denotes the learning rate. The neural network structure to implement such a learning process is shown in Fig. 1, where the first layer performs PCA.

2.4 *ICA neural network with kurtosis optimization*

To start by learning the unknown orthogonal matrix B in Eqn. 5 using a neural network, we denote the estimation of B as the network weight matrix $W = [w_1, w_2, \ldots, w_n]$, where w_i is the ith $n \times 1$ vector. Thus the estimation of the ith source signal $s_i(t)$ can be found by $\hat{s}_i(t) = w_i^T x(t)$. Clearly, $w_1, w_2, \ldots, w_n$ must be orthogonal with one another, which can be guaranteed by adding a orthogonalising routine to the learning procedure of W. Now our task is to learn the n orthogonal weight vectors $w_1, w_2, \ldots, w_n$, based on a certain criterion and learning algorithm, so that $s(t)$ can be estimated from $x(t)$ as well as possible.

Most suggested solutions to blind source separation problems use the fourth-order cumulant or kurtosis of the signals, defined for a zero-mean random variable ξ as

$$kurt(\xi) = E\{\xi^4\} - 3(E\{\xi^2\})^2 \tag{7}$$

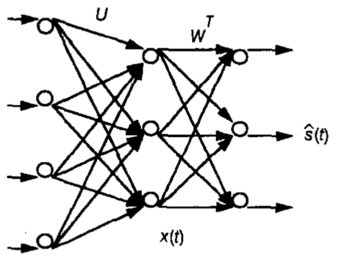

Fig. 1 *Two-layer ICA network: first layer for PCA and second one for estimating B*

Based on eqn. 7, the kurtosis of $\hat{s}_i(t)$ is given by

$$\begin{aligned} kurt(\hat{s}_i(t)) &= kurt(w_i^T x(t)) \\ &= E\{(w_i^T x(t))^4\} - 3[E\{(w_i^T x(t))^2\}]^2 \\ &= e\{(w_i^T x(t))^4\} - 3\|w_i\|_2^4 \end{aligned} \tag{8}$$

where

$$E\{(w_i^T x(t))^2\} = w_i^T E\{x(t)x(t)^T\}w_i = w_i^T w_i = \|w_i\|_2^2$$

and $\|\cdot\|_2$ denotes the 2-norm of a vector. Thus the final objective function is defined as

$$J(w_i) = E\{(w^T x(t))^4\} + F(\|w_i\|_2^2) \tag{9}$$

where F is a scalar function to be determined. The ith weight vector w_i can be updated by the following gradient algorithm:

$$\begin{aligned} w_i^{k+1} &= w_i^k + \mu_i(k)\frac{\partial J}{\partial w_i} \\ &= w_i^k + \mu_i(k) \cdot [\pm x(t)((w_i^k)^T x(t))^3 + f(\|w_i^k\|_2^2)w_i^k] \end{aligned} \tag{10}$$

where k denotes learning time, $\mu_i(k)$ stands for the ith learning rate sequence, and $f = 2F'$. The sign $\pm$ means that a positive sign corresponds to finding the local maxima and a negative sign corresponds to the local minima, which suggests that it is not convenient to use directly the learning algorithm given by eqn. 10. A simple and fast weight-updating algorithm can be derived from eqn. 10, i.e.

$$w_i = \sigma[E\{x(t)(w_i^T x(t))^3\} - 3w_i] \tag{11}$$

where σ is a scalar factor. The fast algorithm for the computation of w is described in Fig. 2 in detail. In Fig. 2, w_i^k denotes the value of the ith weight vector w at time $= k$. $(\cdot)'$ denotes the transpose of a matrix or vector. $E\{\cdot\}$ denotes the expectation of a random variable and is estimated using the mean of the variable in practical computation. The first and second steps express the initialisation process. The fifth step is the vector orthogonalisation process, so that the matrix W finally to be obtained is guaranteed to be orthogonal.

The neural learning process for estimating U and B in eqn. 5, described above, corresponds to the two-layer neural network structure, namely the ICA neural network, as illustrated in Fig 1. It can be seen that the estimation of the source (true) signal vector $\hat{s}(t)$ can be derived from the measurement $v(t)$, a whitening matrix U and an orthogonal matrix W, i.e. $\hat{s}(t) = W^T Uv(t)$, where W is the estimation of B in eqn. 5 ($s(t) = B^T Uv(t)$). The first layer is to perform the PCA of the

(1) Let $i = 0$;
(2) Let $k = 0$ and w_i^0 = a random initial vector and set its 2-norm into 1;
(3) Find $y(t) = x(t)((w_i^k)^T x(t))^3$ and estimate $E\{y(t)\}$ using the mean of $y(t)$, then normalize $E\{y(t)\}$;
(4) Find $w_i^{k+1} = E\{y(t)\} - 3w_i^k$;
(5) If $i = 0$, go to (6), else assume that the previous i weight vectors, $w_0, w_1, \ldots, w_{i-1}$ have been learnt, construct Graml-schmidt orthogonal basis:

$$w_i^{k+1} = w_i^{k+1} - ((w_i^{k+1})^T w_0)w_0 - , \ldots, - ((w_i^{k+1})^T w_{i-1})w_{i-1}$$

(6) Divide w_i^{k+1} by its 2-norm;
(7) If $|(w_i^{k+1})^T w_i^k|$ is not close enough to 1, let $k = k + 1$ and go back to step 3;
(8) $i = i + 1$; if $i < n$ go back to step 2, else stop learning procedure and output all weight vectors:

$w_0, w_1, \ldots, w_{n-1}$.

Fig. 2 *Fast weight-updating algorithm for computation of orthogonal matrix w, i.e. estimation of B in eqn. 5* mixed signals, i.e. turn their correlation matrix into a unit matrix (whitening), so as to simplify the problem to be solved (simplify the problem of finding the arbitrary matrix $\tilde{A}$ in $\hat{s}(t) = \tilde{A}v(t)$ into the problem of finding the orthogonal matrix W in $\hat{s}(t) = W^T Uv(t)$). The simple and effective weight-updating algorithm for the PCA is given by eqn. 6. The second layer is to perform the ICA to recover the source signals from the whitened data. The fast weight-updating algorithm for the ICA is presented in Fig. 2. The learning process of U is completed only when $E\{x(t)x^T(t)\} = I$ is reached, whereas the rule controlling the weight updating of W is that $|W^T W| = 1$. In our experiments, both PCA and ICA algorithms are implemented in MATLAB language. Any other programming language, such as C/C^{++} or Fortran, can also be used, because only some additions and multiplications are involved.

3 Experimental results

First, a validation study was performed to test the efficiency and performance of the proposed ICA neural network. Two groups of simulation data were carefully designed for this purpose. Then, two groups of multichannel EGG data, obtained for humans and dogs, were chosen for the application experiments. All the experiments were performed under MATLAB 4.2 for Windows 3.1/95.

3.1 *Validations*

The first group of verification experiments was designed to test whether the ICA network could perform the BSS accurately. Three-channel simulation signals, with the same length of 30 min and a sampling frequency of 1 Hz, were generated and given, respectively, by $s_1^I(t) = \sin(2\pi \cdot 0.05t)$, simulating 3 cycles min^{-1} gastric slow waves, $s_2^I(t) = \sin(2\pi \cdot 0.2t)$, simulating a 12 cycles min^{-1} respiratory signal, and $s_3^I(t) =$ a random noise, simulating the other interference from the measurement environment. Let s denote the 3×1800 matrix constructed by the three signal vectors, i.e. let $s = [s_1^I \quad s_2^I \quad s_3^I]$ and let the mixing matrix $A = [2.9\ 2.1\ 1.0;\quad 0.22\ 0.2\ 0.2;\ 0.5\ 0.2\ 0.05]$; then the mixed signals, i.e. the simulated observation signals, are obtained by $v = (As)^T$. Fig. 3 shows the three original signals, in which only 120 points (2 min) are displayed for clarity. Fig. 4 illustrates the mixed versions of the three original signals, which intuitively give us nothing but random noise, and, from these mixtures, we cannot imagine which corresponds to the 3 cycles min^{-1} or 12 cycles min^{-1} signal. Only using these mixtures, however, which seem like noise, can the original signals be recovered, using the proposed ICA algorithm described above, which is illustrated in Fig. 5.

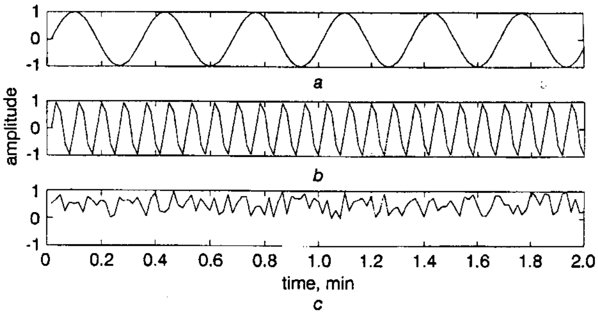

Fig. 3 *Three original simulation signals: (a) 3 cycles min^{-1} signal; (b) 12 cycles min^{-1} signal; (c) random noise*

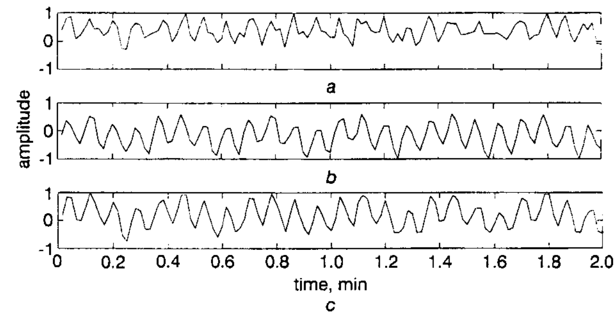

Fig. 4 *Three mixtures of original signals: (a) mixture 1; (b) mixture 2; (c) mixture 3*

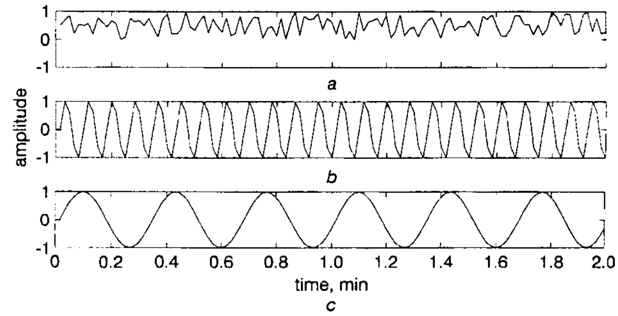

Fig. 5 *Three separated signals: (a) recovered noise; (b) recovered 12 cycles min^{-1} signal; (c) recovered 3 cycles min^{-1} signal*

One of its advantages over single-channel electrogastrography is that multichannel electrogastrography provides information on coupling and propagation. A crucial question is whether the proposed ICA neural network can recover the coupling (frequency) or propagation (phase shift) from observation signals mixed by different frequencies of components and contaminated by environment noises. It was for this purpose that the second group of experiments was carefully carried out.

There were four-channel simulation signals in this group, i.e. standard 3 cycles min^{-1} waves and 2.5 cycles min^{-1} waves, simulating uncoupling, standard 3 cycles min^{-1} waves with 90° phase shift, simulating slow-wave propagation, and random noise. These simulated signals are, respectively, illustrated in Figs. 6*a–d*. Mixing them via a mixture matrix $A = [1\ 3\ 7\ 2;\ 2\ 5\ -3\ 1.2;\ 4\ 7\ 5\ 2.4;\ -0.7\ 1.4\ 2.5\ 0.9]$, we can obtain four mixtures as shown in Fig. 7. Using the neural network shown in Fig. 1 and the corresponding learning algorithms, the four original signals were recovered from these mixed signals, as illustrated in Fig. 8.

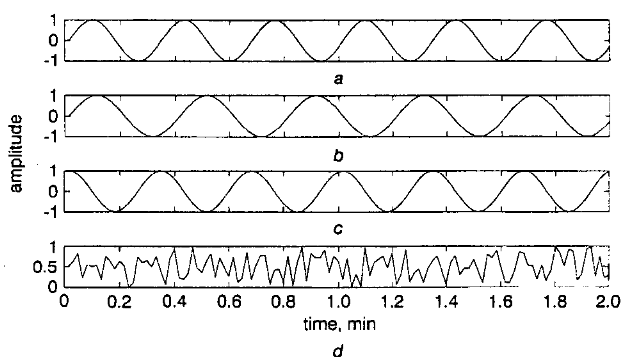

Fig. 6 *Four original simulation signals: (a) 3 cycles min^{-1} signal; (b) 2.5 cycles min^{-1} signal; (c) 3 cycles min^{-1} signal with 90° phaseshift; (d) random noise*

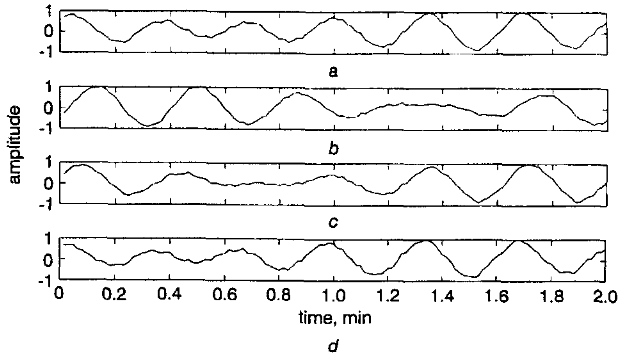

Fig. 7 *Four mixtures of original signals: (a) mixture 1; (b) mixture 2; (c) mixture 3; (d) mixture 4*

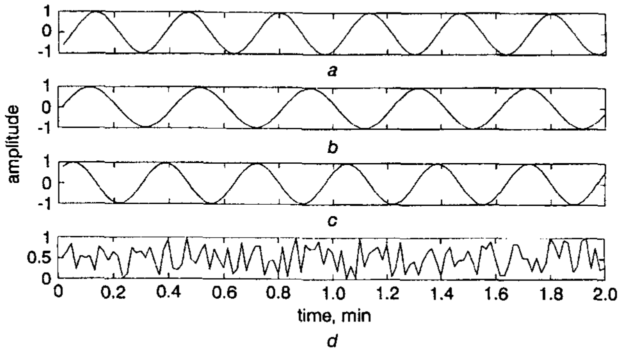

Fig. 8 *Four separated signals: (a) recovered 3 cycles min^{-1} signal; (b) recovered 2.5 cycles min^{-1} signal; (c) recovered 3 cycles min^{-1} signal with 90° phase shift; (d) recovered noise*

To investigate whether the proposed method can recover or keep the frequencies and phase shifts of the original signals, two-dimensional vector analysis (projecting the motion trajectory between two vectors into an *x-y* plane) was performed on the original signals, mixtures and separated signals, as shown in Fig. 9. Fig. 9*a* shows the vector motion trajectory between channel 1 and channel 3 of the original signals, which is a circle because of the same frequency and the 90° phase difference. As far as the mixtures are concerned, every situation for every pair of channels 1 and 2, 1 and 3, 1 and 4, 2 and 3, 2 and 4 and 3 and 4, is illustrated in Figs. 9*b*–*g*, respectively. These complicated patterns show that the mixtures have smeared the characteristics of the frequency and phase of the original signals. As shown in Figs. 8 and 9*h*, the proposed method is not only able to recover the waveforms of the original signals, but also able to keep the frequency and phase shift unchanged after processing. Vector analysis of the processed two-channel signals (channel 1 and channel 3) reveals an unchanged phase shift of 90° (see Fig. 9*h*).

3.2 *Applications*

In the first group of application experiments, three-channel EGGs were recorded from a patient with gastroparesis (male, 39 years old) in the fasting state, using a specially designed multichannel device.* The device consisted of multiple identical amplifiers, each with cutoff frequencies of 1.8 and 16.0 cycles min^{-1}. The device was tested before the study using a multichannel signal generator, and no phase shifts nor time delays were observed among the four channels when an identical sinusoidal signal was sent to the input of each channel. Five electrodes were placed on the abdomen, including three active electrodes (electrodes 1–3), one common reference electrode (electrode 0) and a ground electrode. Electrode 3 was placed 2 cm above the midpoint xiphoid process and umbilicus, and electrodes 2 and 1 were placed 45° upper left to electrode 3, with an interval of 4 cm. Electrode 0 was placed 6–8 cm right horizontal to electrode 1. The three-channel EGG signals were derived by connecting each of the active electrodes to the common reference electrode.

The proposed method was used to process the three-channel EGG signals. The first 10 min of these signals are displayed in Fig. 10. After separation using the ICA network, the three channels of signals become those shown in Fig. 11. Comparing Fig. 10 with Fig. 11, we can easily see that the original three channels are contaminated by artefacts, such as respiration and motion. In the separated signals, however, the artefacts are concentrated on the first and second channels, whereas the third channel is somewhat noise-free.

In the second application, three-channel EGG recordings were made in a healthy dog in the fasting state using a general-purpose multichannel biomedical instrument†. Four paediatric disposable Ag/AgCl electrodes were placed in the epigastric area of the abdomen. Electrodes 1–3 were placed along the middle line, 3 cm apart, and electrode 4, as a common reference, was located at the midpoint. The recording frequency range was 10 Hz, and the signals were sampled at 20 Hz. The reason for using a more general purpose recording device with a wide recording frequency range was to show the efficacy of the proposed method when an imperfect device is used to record EGGs. Fig. 12 shows the first 10 min of the original signals, and Fig. 13 shows those of the signals separated using the proposed ICA network. After processing, artefacts are concentrated on the second and third channels, whereas the first channel is somewhat cleaner. It is shown that a cleaner EGG can be separated out from original multichannel recordings seriously contaminated by ECG and respiration artefacts.

4 Discussion and conclusions

A blind separation method is proposed in this paper for processing multichannel EGGs using neural network-based independent component analysis. In this method, it is assumed that the multichannel EGG recordings result from linear combinations of multiple signal sources, such as gastric signal plus multiple interference, or multiple gastric signals (to be discussed later) plus single or multiple interference, or other combined sources of gastric signals and noise. It is further assumed that the original multiple signal sources are statistically independent. Based on these assumptions, the proposed method can be used to separate these different independent signal sources. It is apparent that the number of channels to be recorded must be equal to or more than the number of independent signal sources.

Unlike traditional methods, such as simple lowpass filtering and advanced adaptive noise cancelling (CHEN, 1989) that are based on some prior information and remove higher-order corrections in the mixtures, the proposed blind source separation method can not only remove frequency-overlapping artefacts, but also does not need any reference signals. This is much closer to practical clinic situations.

In EGG applications, the proposed method can be used to separate the gastric signal from noise and interference and to detect possible multiple gastric signals in the situation of uncoupling of the gastric slow wave. In normal situations,

*Medtronic-Synectics, Shoreview, MN

†AcqKnowledge III, Biopac Systems, Inc.

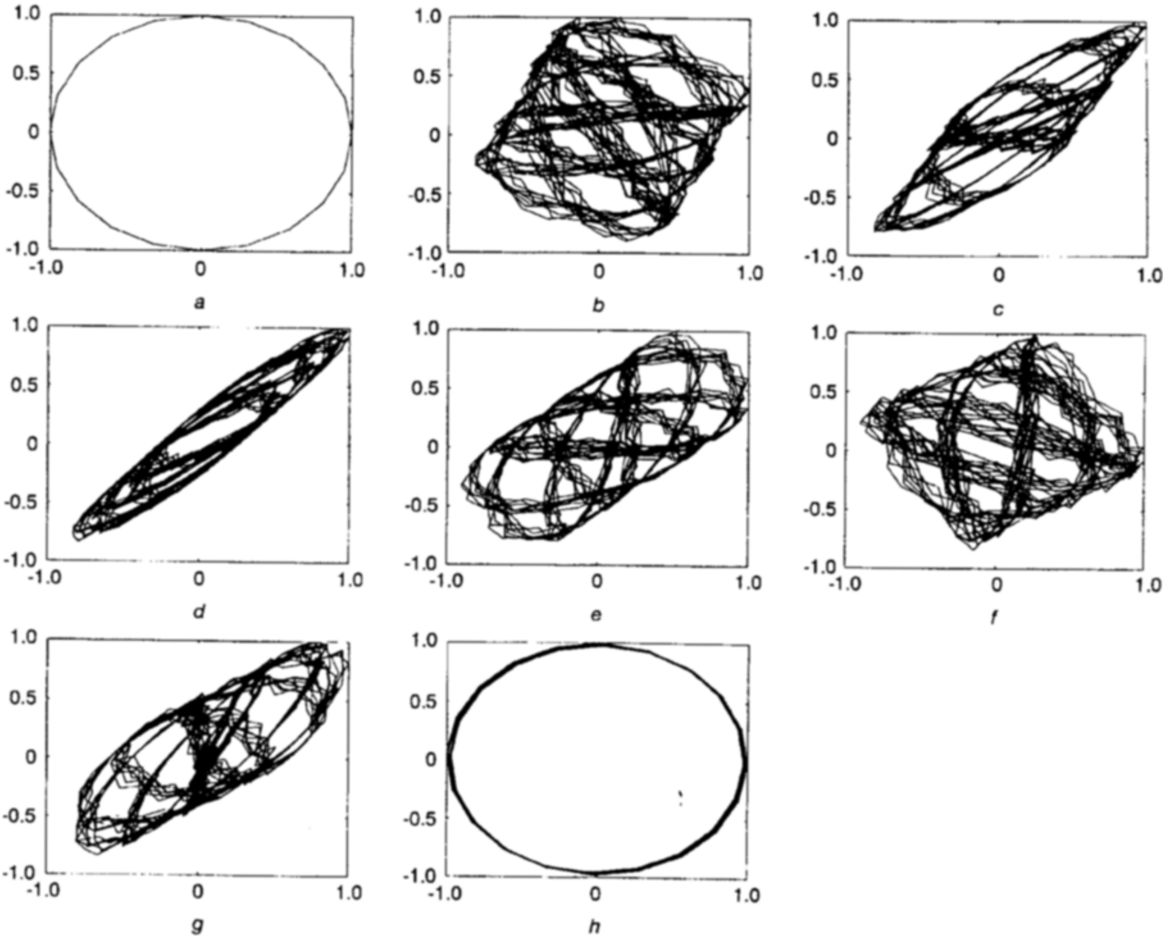

Fig. 9 *Vector analysis (a) for channels 1 and 3 of original signals; (b)–(g) for all combinations of mixed signals: (b) for channels 1 and 2, (c) for 1 and 3, (d) for 1 and 4, (e) for 2 and 3, (f) for 2 and 4, and (g) for 3 and 4; (h) for channels 1 and 3 of recovered signals*

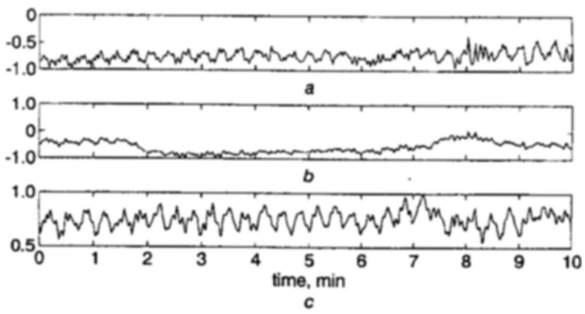

Fig. 10 *Original three-channel EGG of healthy human: (a) channel 1, (b) channel 2, (c) channel 3*

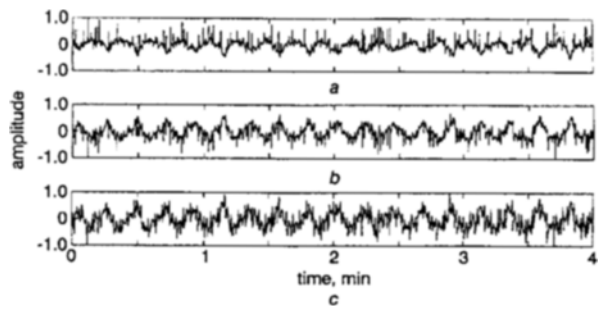

Fig. 12 *Original three-channel EGG of healthy dog: (a) channel 1, (b) channel 2, (c) channel 3*

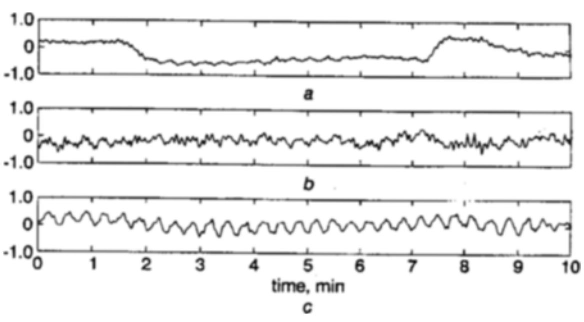

Fig. 11 *Separated three-channel EGG of healthy human. After processing, interference is concentrated on (a) first and (b) second channels, whereas (c) third channel is somewhat noise-free*

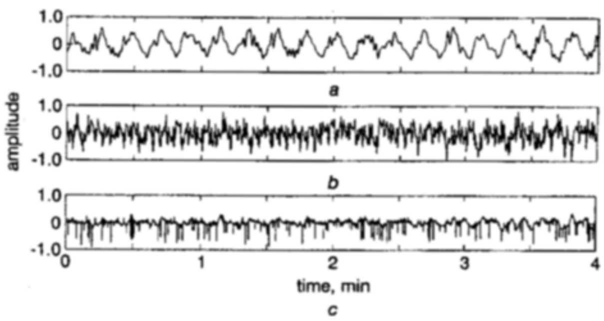

Fig. 13 *Separated three-channel EGG of healthy dog. After processing, artefacts are concentrated on (b) second and (c) third channels, whereas (a) first channel is somewhat cleaner*

the EGG is composed of the gastric slow wave and interference or noise. In a normal stomach, there is only one gastric signal source, i.e. the gastric slow wave, which propagates from the corpus to the pylorus. The interference recorded in the EGG may include motion artefacts, respiration artefacts and ECG artefacts (if the cutoff frequency of the low-pass filter of the amplifier is close to or above 1 Hz). In some cases, myo-electric interference of the small intestine (a frequency of 10–12 cycles $\min^{-1}$) may also be recorded in the EGG. It is apparent that this interference and the gastric slow wave are independent. Therefore, with multichannel recordings of the EGG and the proposed method, the gastric slow wave can be separated from the EGG, as demonstrated by the simulation results shown in Figs. 3–5.

The application experiments presented in this paper focus on removing artefacts from multichannel surface recordings of gastric myo-electric activities with different frequency ranges, recorded from humans and dogs. Also, the simulated experiments suggest that another promising application of the proposed method would be the detection of uncoupling of the gastric slow wave from the EGG. From *in vitro* muscle strip studies, it is known that the smooth muscle of the gastric corpus generates a slow-wave with a frequency of 3 cycles $\min^{-1}$. The smooth muscle of the lower part of the stomach generates a slow wave with a lower frequency. When the stomach is intact, however, the 3 cycles $\min^{-1}$ slow wave generated by the gastric corpus entrains the rest of the stomach and propagates distally towards the pylorus. Consequently, only one gastric slow wave frequency can be recorded from either internal or surface electrodes. In the diseased situation, however, the gastric slow-wave may not be coupled, and thus different areas of the stomach generate gastric slow waves with different frequencies. In addition, it is known that, in some diseased situations, the gastric antrum may generate an ectopic pacemaker of tachygastria (slow-wave frequency too high) and bradygastria (slow-wave frequency too low). When the above abnormalities occur, there are multiple gastric signal sources, and the method proposed in this paper will be able to separate these different gastric signal sources, as shown in Figs. 6–9. Further clinical studies will be performed to show this application.

From the above discussion, it is clear that the proposed method can be used to separate different signal sources. It is therefore not suited to the enhancement of the signal-to-noise ratio of each of the multichannel EGG recordings. This limitation is actually reflected in this paper. As shown in Fig. 12, there are three EGG recordings, each containing regular gastric slow waves mixed with artefacts and random noise. After processing, however, only one channel shows the clean gastric slow wave, whereas the other two represent interference, as shown in Fig. 13. That is, the proposed method is suitable for the separation of independent signal sources (gastric signals and interference), but not adequate for the enhancement of every single channel.

In summary, this paper provides a blind separation method using neural network-based independent component analysis. It is attractive for the separation of the gastric signal from noise in multichannel EGG recordings and for the detection of uncoupled gastric slow waves. Although the paper is focused on EGG applications, the proposed method can also be used for the separation of the signal from noises or detection of multiple signals in other biomedical applications.

References

ALVAREZ, W. C. (1922): 'The electrogastrogram and what it shows', *J.A.M.A.*, **78**, pp. 1116–1118

ABELL, T. L., and MALAGELADA, J. R.. (1988): 'Electrogastrography: current assessment and future perspective', *Dig. Dis. Sci.*, *33*, pp. 982–992

BUREL, G. (1992): 'Blind separation of sources: a nonlinear neural algorithm', *Neural Netw.*, **5**, pp. 937–947

CHEN, J. D. Z., VANDEWALLE, J., VANTRAPPEN, G., and JANSSENS, J. (1989): 'Adaptive method for cancellation of respiratory artifact in electrogastric measurements', *Med. Biol. Eng. Comput.*, **27**, pp. 57–63

CHEN, J. D. Z., and MCCALLUM, R. W. (1993): 'Clinical applications of electrogastrography', *Am. J. Gastroenterol.*, **88**, pp. 1324–1336

CHEN, J. D. Z., and MCCALLUM, R. W. (1994): 'Electrogastrography: Principles and applications' (Raven Press, New York)

CHEN, J. D. Z., LIN, Z. Y., PAN, J., and MCCALLUM. R. W. (1996): 'Abnormal gastric myoelectrical activity and delayed gastric emptying in patients with symptoms suggestive of gastroparesis', *Dig. Dis. Sci.*, **41**, pp. 1538–1545

COMON, P. (1994): 'Independent component analysis, A new concept?', *Signal Processing*, **36**, pp. 287–314

FAMILONI, B. O., KINGMA, Y. J., and BOWES, K. L. (1987): 'Non-invasive assessment of human gastric motor function', *IEEE Trans.* **BME-34**, pp. 30–36

HYVARINEN, A. (1996): 'Simple one-unit neural algorithms for blind source separation and blind deconvolution'. *Proc. Int. Conf. on Neural networks*, Bochum, Germany, **7**, pp. 17–19

JUTTERN, C., and HERAULT, J. (1991): 'Blind separation of sources, Part I: An adaptive algorithm based on neuromimetic Architecture', *Signal Process.*, **24**, pp. 1–10

KOCH, K. L., STERN, R. M., STEWART, W. R., and VASEY, M. W. (1987): 'Electrogastrography: current issues in validation and methodology', *Psychophysiology*, **24**, pp. 55–64

LIANG, J., CHEUNG, J. Y., and CHEN J. D. Z. (1997): 'Detection and deletion of motion artifacts in electrogram using feature analysis and neural networks', *Ann. Biomed. Eng.*, **25**, pp. 850–857

MAKEIG, S., BELL, A. J. (1997): 'Independent component analysis of electroencephalographic data', *Advances in Neural Information Processing System* (MIT Press, Cambridge MA), **8**

MINTCHEV, M. P., KINGMA, Y. J., and BOWES, K. L. (1993): 'Accuracy of cutaneous recordings of gastric electrical Activity', *Gastroenterology*, **104**, pp. 1273–1280

SMOUT, A. J. P. M., VAN DER SCHEE, E. J., and GRASHUIS J. L. (1980): 'What is measured in electrogastrography?', *Dig. Dis. Sci.*, **25**, pp. 179–187

SOROUCHYARI, E. (1991): 'Blind separation of sources, part III: stability analysis', *Signal Process.*, **24**, pp. 21—30

SARNA, S. K. (1975): 'Gastrointestinal electrical activity: terminology', *Gastroenterology*, **68**, pp. 1631–1635

VAN DER SCHEE, E. J., KENTIE, M. A., GRASHUIS, J. L., and SMOUT, A. J. P. M. (1981): 'Adaptive filtering of canine electrogastrographic signals. Part 2: Filter performance', *Med. Biol. Eng. Comput.*, **19**, pp. 765–769

ZHOU, M. Y., ZHANG, H., SHAW, R., and BAMES, F. S. (1997): 'Real-time multichannel computerized electrogastrograph', *IEEE Trans.* **BME-44**, pp. 1228–1236

Author's biography

ZHISHUN WANG received his BSc degree from Beijing University of Posts and Telecommunications, Beijing, China, in 1987, and his MSc degree from Nanjing University of Posts and Telecommunications, Nanjing China, in 1991, all in communications and electronic systems. He received his PhD degree in signals and information processing from Southeast University, Nanjing, China, in 1997. He is currently with Lynn Institute for Healthcare Research, Oklahoma City, OK, USA. His major research interests include biomedical signal/image processing, electrogastrography, biology modeling, neural networks, wavelet, chaos and fuzzy logic.